Preprint Title	DFT Mechanistic Study on the Reaction of Benzenesulfonyl Azides with Oxabicyclic Alkenes
Authors	Daniel A. Akuamoah, Richard Tia and Evans Adei
Publication Date	05 Mai 2020
Article Type	Full Research Paper
Supporting Information File 1	Akuamoah et al_Supporting doc.docx; 149.6 KB
ORCID® iDs	Richard Tia - https://orcid.org/0000-0003-1043-8869

DFT Mechanistic Study on the Reaction of Benzenesulfonyl Azides with Oxabicyclic Alkenes

Daniel Aboagye Akuamoah, Richard Tia* and Evans Adei

Theoretical and Computational Chemistry Laboratory, Department of Chemistry, Kwame Nkrumah University of Science and Technology, Kumasi, Ghana
danielakua99@gmail.com, richardtia.cos@knust.edu.gh/ richtiagh@yahoo.com, eadei@yahoo.com

Abstract

The reaction of benzenesulfonyl azides with oxabicyclic alkenes to form aziridines, reported by Chen et al (*J. Org. Chem.* 2019, 84, 18, 11863-11872), could proceed via initial [3+2] cycloaddition to form triazoline intermediates followed by dinitrogen cleavage or via initial dinitrogen cleavage of the benzenesulfonyl azide to afford a nitrene intermediate followed by insertion of this species into the olefinic bond of the oxabicyclic alkene. Calculations at the DFT M06-2X/6-311G+(d,p) level show that the initial [3+2] cycloaddition has barriers of 17.3 kcal/mol (*endo*) and 10.2 kcal/mol (*exo*) while the initial nitrogen extrusion step has a barrier of 38.9 kcal/mol. The rate-determining step along the former pathway is the dinitrogen cleavage from triazoline cycloadducts which has barriers of 32.3 kcal/mol (*endo*) and 38.6 kcal/mol (*exo*) and that along the latter pathway is dinitrogen cleavage from benzenesulfonyl azide with an activation of barrier of 38.9 kcal/mol. The [3+2] addition of benzenesulfonyl azide with oxabicyclic alkene to afford *endo* and *exo* triazoline intermediates is kinetically favored over the dinitrogen cleavage from benzenesulfonyl azide by 21.6 and 28.1 kcal/mol for *endo* and *exo* pathway respectively. Thus, the preferred pathway for the reaction of oxabicyclic alkene with benzenesulfonyl azide is via initial [3+2] addition followed by dinitrogen cleavage, contrary to the proposal by Chen et al. The lower activation barrier for the dinitrogen extrusion step leading to *endo* aziridine compared to *exo* isomer means that the *endo* product will be formed as the major product, confirming the

experimental observation. The position of substituents on the benzene group of the benzenesulfonyl azide greatly affects the *endo* / *exo* diastereoselectivity.

Keywords: Aziridines, oxabicyclic alkene, benzenesulfonyl azides, triazoline, dinitrogen extrusion, cycloaddition.

1. **Introduction**

Aziridines well-known three-membered heterocycles containing a nitrogen atom, and are among the most widely used intermediates in organic synthesis, where they act as precursors for the synthesis of complex molecules due to the strains incorporated in their skeletons. In addition to their importance as reactive intermediates, many biologically-active compounds have been found to possess these three-membered rings[1–9]. Over 130 biologically active aziridine-containing compounds have been confirmed to have pharmacological activity including antitumor, antibacterial, and antimicrobial effects [10].

Even though aziridines have been synthesized by the reactions of nitrene precursor N-tosyliminobenzyliodinane with olefins, N-tosyliminobenzyliodinane has a short shelf-life and poor solubility in common solvents [11–14]. In 2019, Chen and co-workers successfully reported the synthesis of aziridines by employing a three-component cycloaddition of oxabicyclic alkene with NaN_3 and arylsulfonyl chlorides under metal-free conditions with the aziridine products in good yield up to 82% yield (Scheme 1) [15]. Also, the endo-cycloadduct was obtained as the predominant product, although the cycloaddition of oxabicyclic alkenes have been known to generally produce the exo-product as the predominant product. Chen and co-workers reported that the group positon properties of the monosubstituted arylsulfonyl chlorides had little effect on product yield, but had a large effect on the endo/exo diasterioselectivities of the product; 4-benzenesulfonyl azides gave the endo-cycloadduct as the predominant product whiles 2 or 3-nitrobenzenesulfonyl chloride gave

the exo-cycloadduct as the predominant product. Moreover, electron-withdrawing groups on the oxabicyclic alkene had reduced the product yield but with improved endo-selectively whiles electron-donating groups on the oxabicyclic alkene had slightly higher yields but with decreased endo-selectivity.

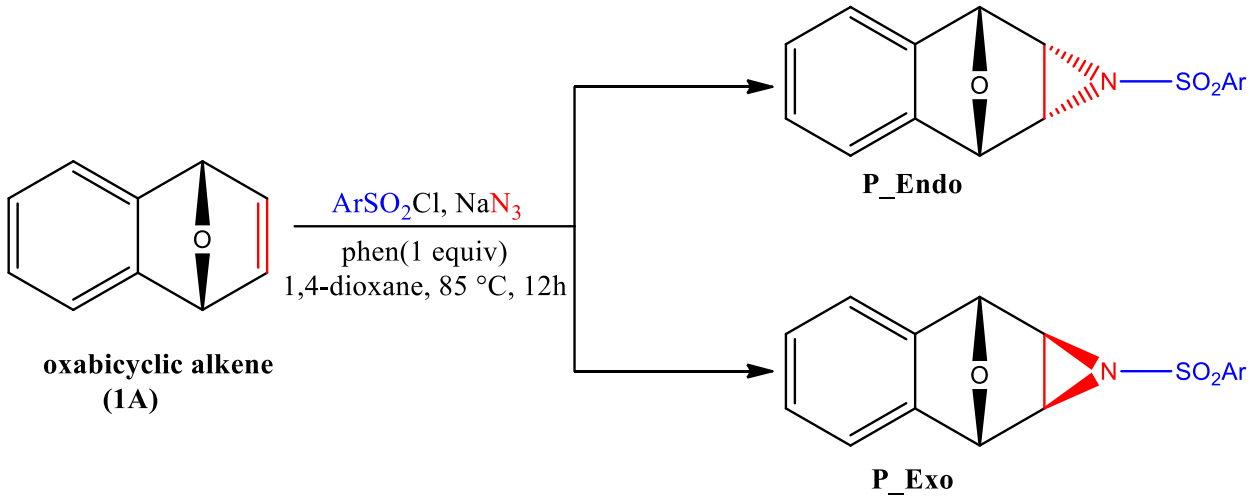

Scheme 1. Three-component cycloaddition of oxabicyclic alkene in the presence of NaN_3 and arylsulfonyl chloride to afford *endo* (**P_Endo**) and *exo* (**P_Exo**) aziridines [15].

Although the products from Chen and co-workers are known, the mechanistic rationale for the observed diasterioselectivities has not been established. After the arylsulfonyl azide has been generated from the reaction of NaN_3 with arylsulfonyl chloride, the plausible mechanism for the reaction of arylsulfonyl azide with oxabicyclic alkene to afford the aziridine products are depicted in **Scheme 2 and 3**. Chen et al. have proposed that the reaction could proceed via an initial dinitrogen cleavage from arylsulfonyl azide to form a nitrene species and subsequent insertion of this species into the olefinic bond of oxabicyclic alkene to afford the aziridine products[15]. However, the reaction could also proceed via [3+2] cycloaddition to afford triazoline intermediates and subsequent dinitrogen cleavage from this intermediate to form the final aziridine products. Which pathway is preferred? Computational chemistry methods are often employed in the

prediction and rationalization of reactivity trends in order to provide theoretical guidance for correlative experiments.

Herein, density functional theory (DFT) calculations are employed to elucidate the mechanism of the reaction of arylsulfonyl azides with oxabicyclic alkene toward the formation of aziridines. The aim of this study is to provide a detailed mechanistic insight into the reaction of arylsulfonyl azides with oxabicyclic alkene by examining the energetics of the various elementary steps leading to the formation of the observed exo/endo products in the experimental work of Chen et al [15]. The effect of different substituents on the benzene group of the benzenesulfonyl azide and on the oxabicyclic alkene on the energetics of the reaction is also investigated. In addition, the effect of solvent on the energetics of the reaction is also explored. An in-depth understanding of the mechanism of the reaction will provide chemical insights into the reactivity of the reaction which is crucial for the control and development of better synthetic methods to influence product outcomes.

Path A

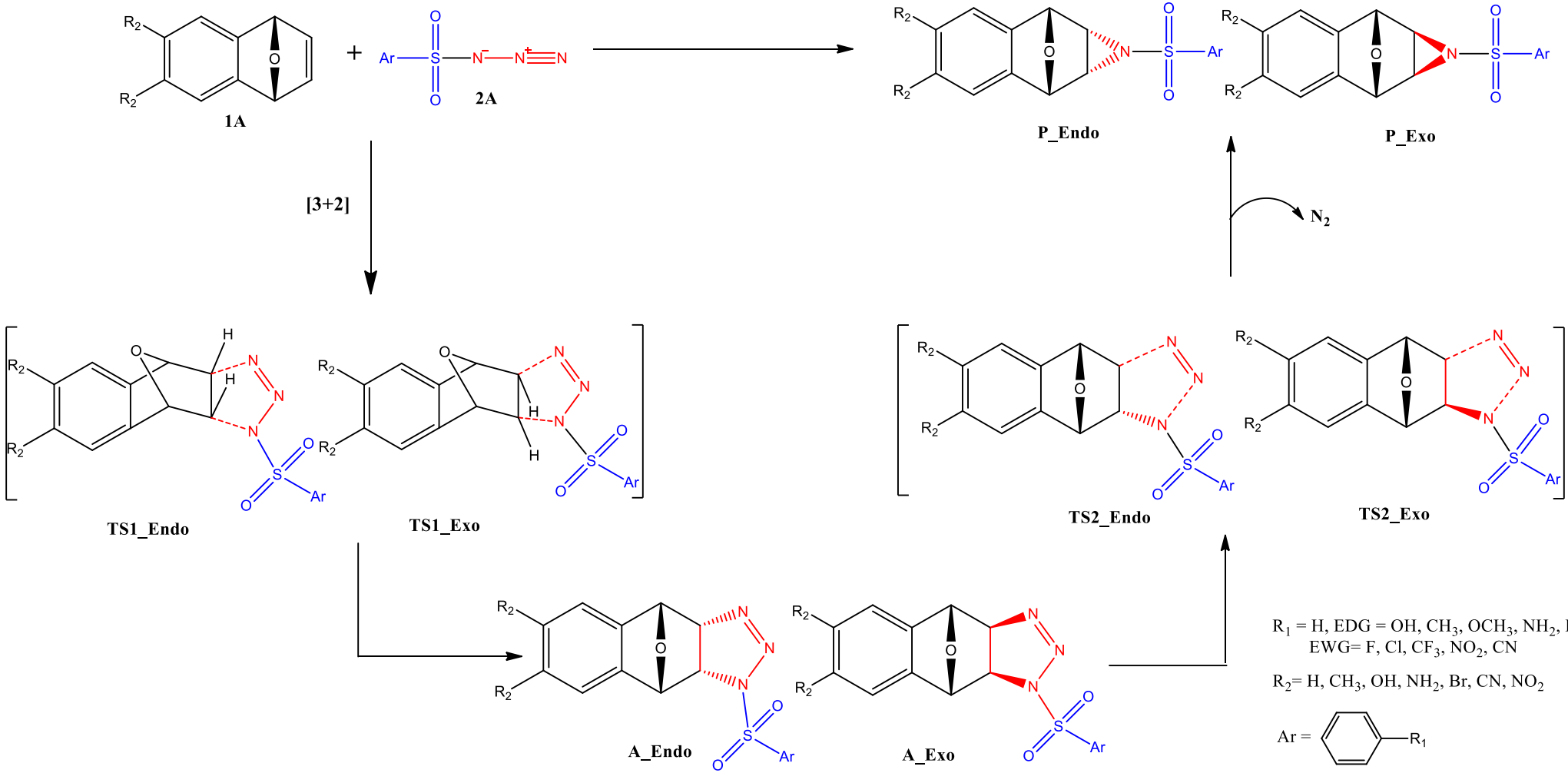
1A
2A
[3+2]
P_Endo
P_Exo
N2
TS1_Endo
TS1_Exo
TS2_Endo
TS2_Exo
A_Endo
A_Exo
R1 = H, EDG = OH, CH3, OCH3, NH2, Ph
EWG= F, Cl, CF3, NO2, CN
R2= H, CH3, OH, NH2, Br, CN, NO2
Ar =

Scheme 2. Proposed reaction pathway for the reaction of oxabicyclic alkene **1A** and arylsulfonyl azide **2A** to afford aziridines **P_Endo** and **P_Exo** via **Path A**.

Path B

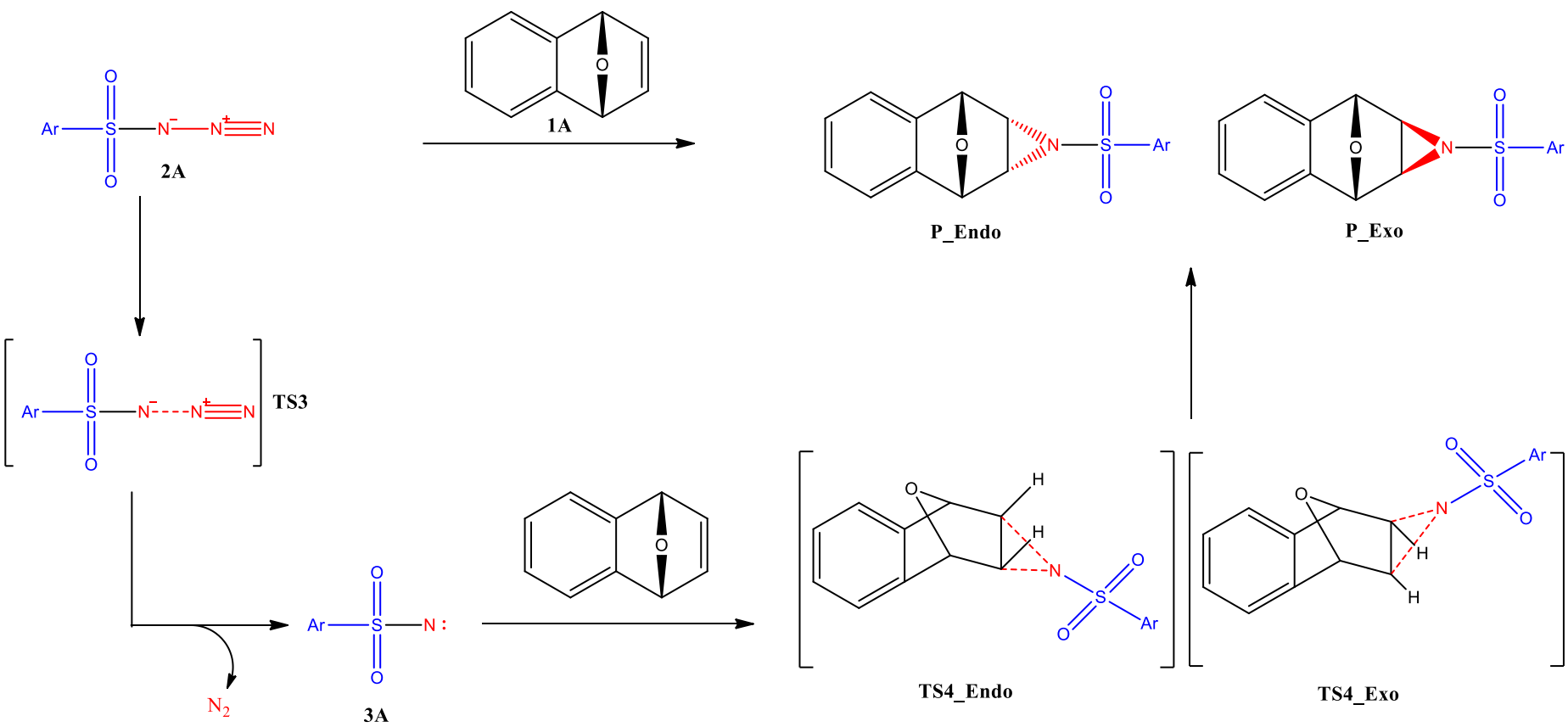

Scheme 3. Proposed reaction pathway for the reaction of Oxabicyclic alkene **1A** and arylsulfonyl azide **2A** to afford aziridines **P_Endo** and **P_Exo** via **Path B** [15].

2. Computational details and methodology

All the quantum chemical calculations were carried out with the Spartan'14[16] and Gaussian 09[17] computational chemistry software suites at the M06-2X/6-311+G(d,p) levels of theory. The Minnesota functional M06-2X, developed by Zhao and Truhlar [18], is a hybrid meta-generalized gradient approximation (meta-GGA) functional that has been shown to be effective at geometry optimizations and computing thermochemical and kinetic parameters of chemical reactions[19,20]. Using the polarizable continuum model (PCM), 1,4-dioxane was employed to compute solvation effects in the reactions [21].

The guess geometries of the molecules were constructed with the Spartan's graphical model builder and minimized interactively using the molecular mechanics force field [22]. Transition state structures were computed by first obtaining guess input structures. This was achieved by constraining specific internal coordinates of the molecules (bond lengths, bond angles, dihedral angles) while fully optimizing the remaining internal coordinates. This procedure gives appropriate guess transition state input geometries which are then submitted for full transition state calculations without any geometry or symmetry constraints.

Full harmonic vibrational frequency calculations were carried out to verify that each transition state structure had a Hessian matrix with only a single negative eigen value, characterized by an imaginary vibrational frequency along the respective reaction coordinates. Intrinsic reaction coordinate calculations were then performed to ensure that each transition state smoothly connects the reactants and products along the reaction coordinate [23,24].

The global electrophilicities (ω), and maximum electronic charge (ΔN_{max}) of the various benzenesulfonyl azide derivatives were calculated using equations (1) and (2). The electrophilicity index measures the ability of a reactant to accept electrons [25] and it has been found to be a function of the electronic chemical potential, $\mu = (E_{HOMO} + E_{LUMO})/2$ and chemical hardness, $\eta = (E_{LUMO} - E_{HOMO})$ as defined by Pearson's acid-base concept [26]. Hence, species with large electrophilicity

values are more reactive towards nucleophiles. These equations are based on the Koopmans theory [27] originally established for calculating ionization energies from closed-shell Hartree–Fock wavefunctions, but have since been adopted as acceptable approximations for computing electronic chemical potential and chemical hardness.

$$\omega = \mu^2/2\eta \qquad (1)$$

$$\Delta N_{max} = -\mu/\eta \qquad (2)$$

The maximum electronic charge transfer (ΔN_{max}) measures the maximum electronic charge that the electrophile may accept. Thus, species with large ΔN_{max} index would be best electrophile and hence poor nucleophile given a series of compounds.

3.0 Results and discussion

Based on scheme 2 and 3, the reaction of oxabicyclic alkene **1A** with benzenesulfonyl azide have been studied at the M06-2X/6-311G+(d,p) level of theory. The formation of products **P_Endo** and **P_Exo** was proposed by Chen and co-workers to occur via an initial dinitrogen extrusion from benzenesulfonyl azide **2A** to afford intermediate **3A** through **TS3**. Intermediate **3A** then inserts into the olefinic bond of the oxabicyclic alkene through **TS4_Endo** and **TS4_Exo** to afford products **P_Endo** and **P_Exo** respectively [15]. Based on some preliminary calculations, we proposed an alternative pathway for the reaction of oxabicyclic alkene with benzenesulfonyl azide. We propose that the formation of **P_Endo** and **P_Exo** occur also via an initial [3+2] cycloaddition fashion or 1,3-dipolar cycloaddition reaction between the benzenesulfonyl azide and the oxabicyclic alkene to afford intermediates **A_Endo** and **A_Exo** through **TS1_Endo** and **TS1_Exo** respectively. Intermediates **A_Endo** and **A_Exo** then undergo dinitrogen cleavage or extrusion through **TS2_Endo** and **TS2_Exo** to afford products **P_Endo** and **P_Exo** as depicted in scheme 2.

The results of the reaction of oxabicyclic alkene with benzenesulfonyl azide in the gas phase and the effect 1,4-dioxane solvent on the energetics of the reaction are discussed in Section 3.1 and 3.2 respectively. The effect of electron-donating groups and electron-withdrawing groups on the benzene moiety of the benzenesulfonyl azide on the reaction of oxabicyclic alkene with benzenesulfonyl azide are discussed in section 3.3. The reaction of 4-nitrobenzenesulfonyl and 4-methoybenzenesulfonyl azide with several di-substituted oxabicyclic alkenes are discussed in section 3.4. Section 3.5 discusses the change in regioselectivity when 2 or 3-substituted-benzenesulfonylazide is employed. Section 3.6 deals with the orbital interactions between benzenesulfonyl azide and oxabicyclic alkene, while the global reactivity indices for the various oxabicyclic alkenes and benzenesulfonyl azides are discussed in Section 3.7. All the energies reported herein are Gibbs free energy with zero-point corrections.

3.1 **Reaction of oxabicyclic alkene and benzenesulfonyl azide to afford aziridines P_Endo and P_Exo**

The relative energies of the reactants, intermediates, transition states and products as well as optimized geometries of the transition state structures involved in the reaction of oxabicyclic alkene with benzenesulfonyl azide are shown in Figure 1 and Figure 2 respectively. For **Path B**, in the first step of the reaction, benzenesulfonyl azide undergoes dinitrogen extrusion through **TS3** with an activation barrier of 38.9 kcal/mol and reaction energy of 11.8 kcal/mol leading to the formation of intermediate **3A**. Intermediate **3A** then inserts itself into the olefinic bond of the oxabicyclic alkene as shown in Scheme 2 through **TS4_Endo** and **TS4_Exo** with activation barriers of 4.3 and 4.3 kcal/mol respectively leading to the formation of products **P_Endo** and **P_Exo**. This pathway is not selective towards any of the products.

In our proposed pathway (**Path A**), we observed that the [3+2] addition reaction of benzenesulfonyl azide with the oxabicyclic alkene through **TS1_Endo** and **TS1_Exo** is kinetically favored with an activation barrier of 17.3 and 10.8 kcal/mol leading to the formation of

intermediate **A_Endo** and **A_Exo** respectively. Moreover, formation of intermediates **A_Endo** and **A_Exo** is exergonic and thermodynamically favored by -42 and -43.5 kcal/mol respectively. The stability of **A_Endo and A_Exo** reveal that intermediates **A_Endo** and **A_Exo** should be observed in the reaction. Intermediates **A_Endo** and **A_Exo** then undergo dinitrogen extrusion through **TS2_Endo** and **TS2_Exo** with activation energies of 32.3 and 38.6 kcal/mol. Formation of products **P_Endo** through **TS2_Endo** is kinetically favored over formation of **P_Exo** via **TS2_Exo** by 6.6 kcal/mol. From the results, the rate-determining step for the formation of products **P_Endo** and **P_Exo** is the dinitrogen extrusion from intermediates **A** as depicted in Scheme 2. Although the formation of intermediate **A_Exo** is kinetically favored over the formation of intermediate **A_Endo**, the overall formation of products **P_Endo** and **P_Exo** is controlled by the dinitrogen cleavage step which is the rate-determining step of this reaction hence **P_Endo** will be formed in greater yield than **P_Exo**. This accounts for observations made by Chen and co-workers in their experimental work where **P_Endo** was isolated as the major product and **P_Exo**, the minor product. Our results indicate that the most feasible pathway for the formation of products **P_Endo** and **P_Exo** is through **Path A** and not **Path B**, looking at the energetics of the reaction.

It should be noted that [3+2] addition of benzenesulfonyl azide with oxabicyclic alkene to afford intermediates **A_Endo** and **A_Exo** is kinetically feasible over the dinitrogen cleavage from benzenesulfonyl azide by 21.6 and 28.1 kcal/mol for *endo* and *exo* pathway respectively. Also, formation of intermediates **A_Endo** and A**_Exo** is thermodynamically favoured over the formation of intermediate **3A** by 54.3 and 55.3 kcal/mol respectively. Although the subsequent insertion of intermediate **3A** into the olefinic bond of the oxabicyclic alkene is kinetically and thermodynamically feasible, the energetics show that intermediates **A_Endo** and **A_Exo** would be formed quickly over intermediate **3A** rendering the formation of intermediate **3A** less likely to occur. Moreover, the products distribution of **P_Endo** and **P_Exo** would be even if the reaction

is to go through **Path B** since the activation barrier for reaction of intermediate **3A** with oxabicyclic alkene is 4.3 and 4.3 kcal/mol for **TS4_Endo** and **TS4_Exo** respectively but an even product distribution is not observed, hence the most feasible pathway for the formation of aziridines **P_Endo** and **P_Exo** for the reaction of oxabicyclic alkene with benzenesulfonyl azides is through **Path A** and not **Path B**.

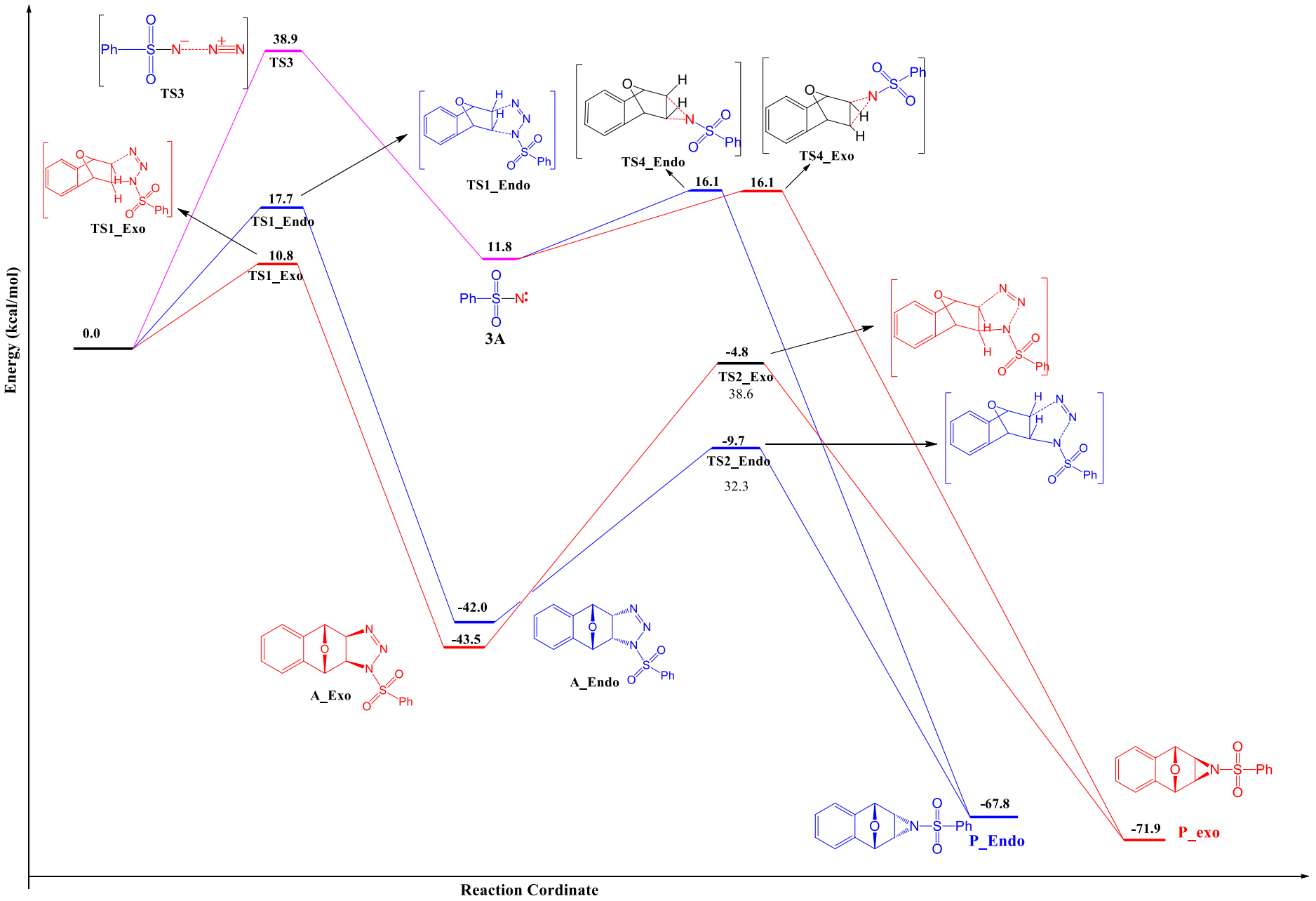

Figure 1 Zero-point energy corrected Gibbs free energy profile for the reaction of Oxabicyclic alkene and benzenesulfonyl azide to afford Aziridines P_Endo and P_Exo. All stationary points are optimized at the M06-2X/6-311G+(d,p) level of theory at 85 °C in gas phase. Relative energies in kcal/mol.

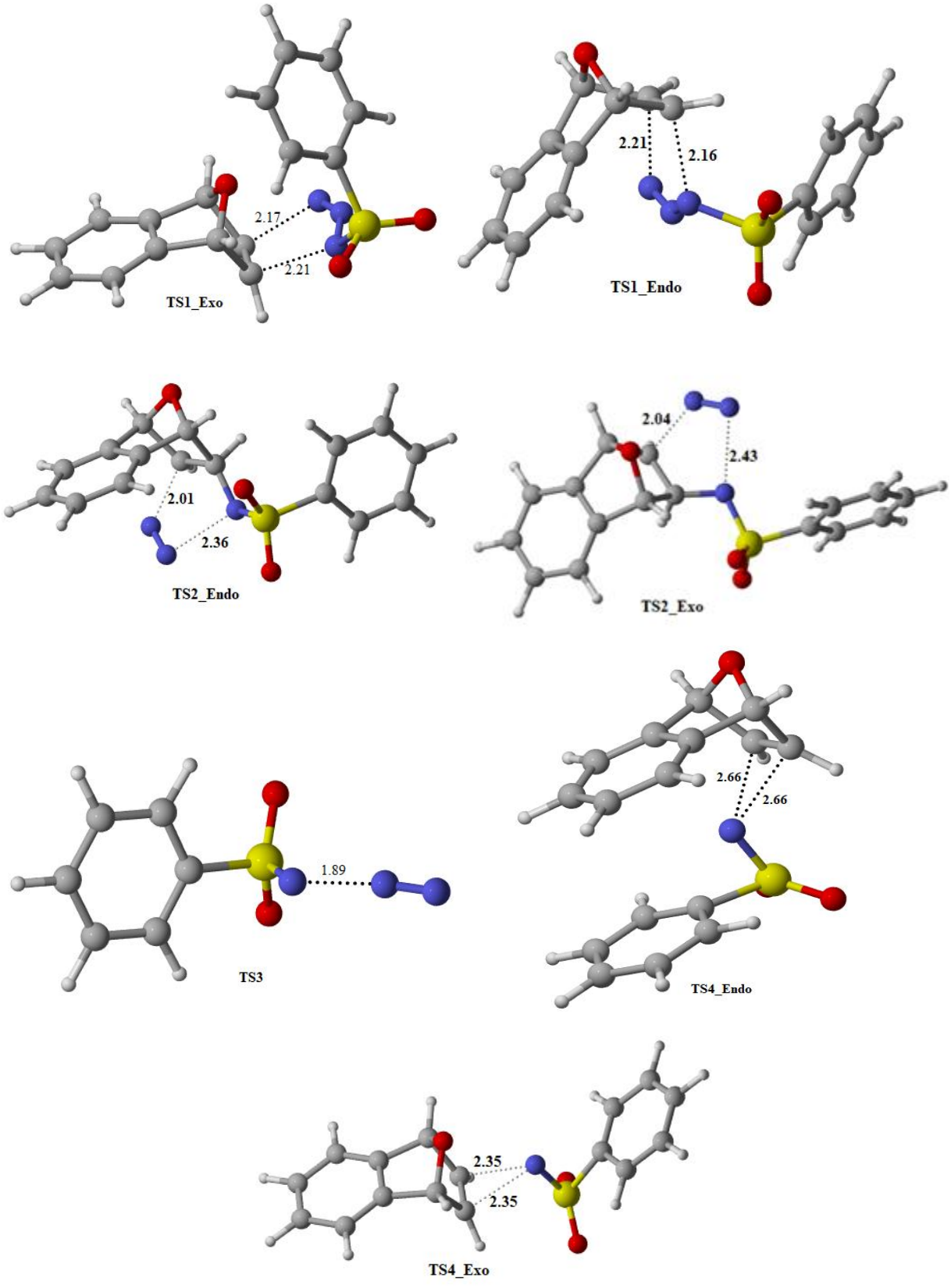

Figure 2. Gas phase optimized geometries of possible transition state structures involved in reaction of oxabicyclic alkene with benzenesulfonyl azide as calculated by M06-2X/6-311+G(d,p) at 85 °C. Bond lengths are in Å.

3.2.1 Effects of solvent 1,4-dioxane on the energetics of the reaction

Using the polarizable continuum model (PCM), the effect of solvent 1,4-dioxane on the energetics of the reaction of oxabicyclic alkene with benzenesulfonyl azide was investigated. There appears to be a minimal solvent effect on **Path B**. 1,4-dioxane marginally reduces the activation barrier of the dinitrogen cleavage from benzenesulfonyl azide through **TS3** by 1.2 kcal/mol. Also the activation barrier for the insertion of the nitrene species (intermediate **3A**) into the olefinic bond of oxabicyclic alkene is 4.2 (endo) and 4.0 kcal/mol (exo) in 1,4-dioxane. With these results, we can still infer that the product distribution of **P_Endo** and **P_Exo** should be even if the reaction is to proceed via **Path B**.

Along **Path A**, 1,4-dioxane marginally increase the activation barrier of the [3+2] addition step through **TS1_Endo** and **TS1_Exo** by 0.4 and 0.6 kcal/mol respectively. Moreover, 1,4-dioxane slightly reduces the activation barrier for the dinitrogen extrusion step through **TS2_Endo** and **TS2_Exo** by 2.0 and 2.3 kcal/mol respectively. The activation barrier of the dinitrogen extrusion step via **TS2_Endo** and **TS2_Exo** is 29.8 and 36.0 kcal/mol respectively. In 1,4-dioxane, formation of products **P_Endo** through **TS2_Endo** is kinetically favored over formation of **P_Exo** via **TS2_Exo** by 6.2 kcal/mol compared to 6.3 kcal/mol in the gas phase. Although there are slight variations in the activation barriers, the energetic trends remain unchanged hence gas phase calculations are deemed adequate for the reactions studied.

Table 1. Activation energies of the elementary steps involved in the reaction of benzenesulfonyl azide and oxabicyclic alkene, computed at the M06-2X/6-311+G(d,p) level of theory. Energies in kcal/mol. Energies in bracket were computed at M06-2X/6-311G(d,p) level.

Medium	TS1_Endo	TS1_Exo	TS2_Endo	TS2_Exo	TS3	TS4_Endo	TS4_Exo
Gas Phase	17.3	10.8	32.3 (31.9)	38.6 (38.3)	38.9	4.3	4.3
1,4-Dioxane	17.7	11.5	30.3 (29.8)	- (36.0)	37.3	4.2	4.0

Table 2. Relative energies of intermediates and products involved in the reaction benzenesulfonyl azide and oxabicyclic alkene, computed at the M06-2X/6-311+G(d,p) level of theory. Energies in kcal/mol.

Medium	**1A + 2A**	**A_Endo**	**A_Exo**	**3A + N_2**	**P_Endo+N_2**	**P_Exo+N_2**
Gas Phase	0.0	-42.0	-43.5	11.8	-67.8	-71.7
1,4-Dioxane	0.0	-41.6	-43.5	13.4	-67.8	-71.9

3.2.2 Product distribution in the reaction of oxabicyclic alkene with benzenesulfonyl azide

The Boltzmann distribution has been applied to rationalize the amount of **P_Exo** and **P_Endo** that will be formed in the reaction of benzenesulfonyl azide with oxabicyclic alkene using the energetics obtained. Here, the activation barrier for the rate-determining step is employed. The ratio of *endo* to *exo* products can be written as:

$$\frac{P\text{endo}}{Pexo} = \exp\left(\frac{E\text{exo} - E\text{endo}}{kT}\right)$$

Since **TS2_Exo** – **TS2_Endo** = 6.3 kcal/mol, T = 358.15 K, and *k* = 18(0.0019872014) kcal/mol.K

$$\frac{P\text{endo}}{Pexo} = \exp\left(\frac{6.3\ kcal/mol}{\frac{18(0.0019872014)kcal}{molK} * 358.15K}\right)$$

$$\frac{P\text{endo}}{Pexo} = \exp(0.492)$$

$$\frac{P\text{endo}}{Pexo} = 1.64 = \frac{62.1}{37.9} \approx 62:38$$

The experimentally-observed product distribution from the work of Chen et al [15] in the reaction of benzenesulfonyl azide with oxabicyclic alkene for *endo*: *exo* is 67:33, and this is in excellent agreement with our computed results.

3.3 Substituent effects on the reaction of oxabicyclic alkene with benzenesulfonyl azide

To investigate the effects of substituents on the energetics of the reaction and products outcomes, electron-donating groups and electron-withdrawing groups are introduced at the position R1 of the benzene group on the benzenesulfonyl azide. The aim of this section of the study is to predict the type of substituents that the benzenesulfonyl azide substrate must contain to influence products yield. The results obtained under this section of the study are reported in Table 3 to 7.

3.3.1 Effect of electron-donating groups on the reaction

To establish the effects of electron-donating groups (EDGs) on the energetics of the reaction, we employed Ph, CH_3, OCH_3, OH, and NH_2 substituted benzenesulfonyl azide. In all cases a marginal decrease in activation barriers for the initial [3+2] addition step through **TS1_EN** compared to the parent reaction is observed, with Ph and CH_3 having the least activation barrier of 17.1 kcal/mol indicating a decrease by 0.2 kcal/mol, and OCH_3, OH, and NH_2 having activation barriers of 17.2 each. With the exception of NH_2, a marginal increase in activation barriers is also observed for the initial [3+2] cycloaddition addition leading to the formation of intermediates **A_Exo** through **TS1_Exo**. OH has the least activation barrier of 10.5 kcal/mol for the cycloaddition step through **TS1_Ex** indicating a marginal increase of 0.3 kcal/mol. The observed trend for **TS1_Ex** is OH < Ph < OCH_3 < CH_3 < NH_2. A general increase in activation barrier for dinitrogen extrusion step through **TS2_Endo** and **TS2_Exo**, the rate-determining step for the formation of products **P_Endo** and **P_Exo**, is observed in all cases. The trend for **TS2_Endo** is Ph < OH < CH_3 < OCH_3 < NH_2 with Ph having an activation barrier of 32.4 kcal/mol indicating an increase by 0.1 kcal/mol and NH_2 having an activation barrier of 33.3 kcal/mol, an increase by 1.0 kcal/mol. The observed trend for **TS2_Exo** leading to the less favored product is also Ph < OH < CH_3 < OCH_3 < NH2 with Ph and NH_2 having activation barriers of 38.6 and 39.5 kcal/mol indicating a marginal increase by 0.1 and 0.9 kcal/mol respectively.

Also, the effect of OH and OCH_3 on the reaction via **Path B** was also investigated. A marginal decrease in activation barrier for initial dinitrogen extrusion is observed for both OH and OCH_3 with OH and OCH_3 having activation barriers of 37.1 kcal/mol and 37.0 kcal/mol respectively. Also the activation barriers for the nitrene insertion into the olefinic bond for OH and OCH_3 substituents are 3.1 kcal/mol (*endo* and *exo*) and 3.2 kcal/mol (*endo* and *exo*). With these results, distribution of *endo* and *exo* products is expected to be even if the reaction is to proceed via **Path B** but an even product distribution is not observed in experiment.

3.3.2 Effect of electron-withdrawing groups on the reaction

In order to establish the effect of electron-withdrawing groups (EWGs) on the energetics of the reaction, we employed F, Cl, CF_3, CN, and NO_2 substituted benzenesulfonyl azide. In all cases, a marginal decrease in activation barrier is observed for **TS1_Endo** and **TS1_Exo** (see table 3), with NO_2 having the least activation barrier of 16.8 and 9.3 kcal/mol for **TS1_Endo** and **TS1_Exo** respectively. The observed trend for **TS1_Endo** is NO_2 < CN < CF_3 < Cl < F. The same trend is also observed for **TS1_Exo**. Also the activation barrier for the di-nitrogen extrusion step through **TS2_Exo** and **TS2_Exo** is reduced owing to the presence of these EWGs, with NO_2 having the least activation barrier of 30.2 and 35.8 kcal/mol for **TS2_Exo** and **TS2_Endo** indicating a decrease by 2.1 and 2.8 kcal/mol respectively. In all cases for both electron-donating and electron-withdrawing groups, at the para-position or position 3 of the benzene group on the benzenesulfonyl azide, dinitrogen-extrusion via **TS2_Endo** is more favored than dinitrogen extrusion via **TS2_Exo**.

The effect of Cl, F, CN, and NO_2 on the energetics of the reaction via **Path B** was also investigated. For CN and NO_2, a marginal increase in activation barrier is observed for the initial nitrogen extrusion via **TS3** with CN and NO_2 having activation barriers of 39.1 and 39.4 kcal/mol respectively and a marginal decrease is observed for CN and NO_2 with activation barriers of 38.0

and 38.3 kcal/mol respectively. In all cases the activation barrier for dinitrogen extrusion via **TS3** which is the rate-determining step via **Path B** is higher than the barrier for dinitrogen extrusion via **TS2_Endo** and **TS2_Exo** which the rate-determining step via **Path A**. This results also indicate that, the most feasible pathway for the reaction of oxabicyclic alkene with arylsulfonyl azides is via **Path A** and not **Path B**.

Table 3. Activation energies of the elementary steps involved in the reaction of Ph-, CH_3-, OCH_3-, OH-, and NH_2-substituted benzenesulfonyl azide and oxabicyclic alkene, computed at the M06-2X/6-311+G(d,p) level of theory. Energies in kcal/mol.

Substituents	TS1_Endo	TS1_Exo	TS2_Endo	TS2_Exo
Ph	17.1	10.6	32.4	38.7
CH_3	17.1	10.8	32.6	38.9
OCH_3	17.2	10.7	32.9	39.1
OH	17.2	10.5	32.6	38.8
NH_2	17.2	11.0	33.3	39.5

Table 4. Relative energies of intermediates and products involved in the reaction of Ph-, CH_3-, OCH_3-, OH-, and NH_2-substituted benzenesulfonyl azide and oxabicyclic alkene, computed at the M06-2X/6-311+G(d,p) level of theory. Energies in kcal/mol.

Substituents	1A + 2A	A_Endo	A_Exo	P_Endo	P_Exo
Ph	0.0	-42.1	-43.7	-68.0	-71.8
CH_3	0.0	-41.9	-43.5	-67.5	-71.6
OCH_3	0.0	-41.9	-43.6	-67.8	-71.6
OH	0.0	-42.0	-43.7	-68.0	-71.8
NH_2	0.0	-41.7	-43.1	-67.3	-71.3

Table 5. Activation energies of the elementary steps involved in the reaction of F-, Cl-, CF_3-, CN-, and NO_2-substituted benzenesulfonyl azide and oxabicyclic alkene at the M06-2X/6-311+G(d,p) level of theory. Energies in kcal/mol.

Substituents	TS1_Endo	TS1_Exo	TS2_Endo	TS2_Exo
F	17.1	10.2	31.9	38.0
Cl	17.1	10.2	31.7	37.8
CF3	16.9	9.7	30.9	37.1
CN	16.9	9.6	30.6	36.1
NO2	16.8	9.3	30.2	35.8

Table 6. Relative energies of intermediates and products involved in the reaction of F-, Cl-, CF_3-, CN-, and NO_2-substituted benzenesulfonyl azide and oxabicyclic alkene at the M06-2X/6-311+G(d,p) level of theory. Energies in kcal/mol.

Substituents	1A + 2A	A_Endo	A_Exo	P_Endo	P_Exo
F	0.0	-42.4	-44.1	-68.5	-72.4
Cl	0.0	-42.4	-44.2	-65.6	-72.3
CF3	0.0	-42.8	-44.6	-69.0	-72.8
CN	0.0	-42.8	-44.7	-69.3	-72.9
NO2	0.0	-43.0	-45.0	-69.6	-73.1

Table 7. Activation energies of the elementary steps involved in the reaction of OH-, OCH_3, F-, Cl-, CN-, and NO_2-substituted benzenesulfonyl azide and oxabicyclic alkene via Path B at the M06-2X/6-311+G(d,p) level of theory. Energies in kcal/mol.

Substituents	TS3	TS4_Endo	TS4_Exo
H	38.9	4.3	4.3
OH	37.1	3.1	3.1
OCH3	37.0	3.2	3.2
F	38.0	3.4	3.6
Cl	38.3	3.3	3.7
CN	39.1	3.0	3.4
NO2	39.4	2.7	3.4

3.4 Reaction of di-substituted oxabicyclic alkenes with benzenesulfonyl azides

This section of the study investigates how substituents on the oxabicyclic alkene affect the reactivity of oxabicyclic alkenes with benzenesulfonyl azides. 4-nitrobenzenesulfonyl azide and 4-methoxybenzenesulfonyl azide which have very strong electron-withdrawing and electron-donating groups were employed, and substituents were varied on the oxabicyclic alkene. The results of this section of the study are tabulated in tables 8 to 11 and discussed below.

Our results indicate that when electron-donating groups are substituted at the position 6 and 7 of the oxabicyclic alkene, rendering it electron-rich, the activation barrier for the initial cycloaddition step through **TS1_Exo** and **TS1_Endo** is reduced. Electron-donating groups employed in this section of the study are CH_3, OH, and NH_2. A significant decrease in activation barrier for **TS1_Endo** is observed with OH having the least activation barrier of 12.0 kcal/mol indicating a decrease by 4.8 kcal/mol, followed by NH_2 and CH_3 with activation barriers of 12.1 and 16.3 kcal/mol respectively. It is important to note that electron-donating groups also decrease the activation barrier for the cycloaddition step through **TS1_Exo**, hence favoring the formation of the exo product too. There appears to be no significant effect on the activation barriers of the dinitrogen extrusion step via **TS2_Endo** and **TS2_Exo** since the change in activation barriers are within the range of 0 to 0.9 kcal/mol. The decrease in activation barrier of **TS1_Exo** and

TS1_Endo may correspond to slight increase in product yield but with decreased selectivity since the exo-product is also favoured.

On the other hand, electron-withdrawing groups at the position 6 and 7 of the oxabicyclic alkene significantly decrease the activation barrier of the cycloaddition addition through **TS1_Endo** and increase the activation barrier for **TS1_Exo**, with NO_2 having an activation barrier of 13.7 kcal/mol and 11.6 kcal/mol for **TS1_Endo** and **TS1_Exo** respectively. This corresponds to a decrease by 3.1 kcal for **TS1_Endo** and an increase by 1.0 kcal/mol for **TS1_Exo**. The observed trend for **TS1_Endo** is NO_2 < Br < CN, with Br and CN having an activation barrier of 14.4 and 14.6 kcal/mol indicating a decrease by 2.4 and 2.2 kcal/mol respectively. The increase in activation barrier for **TS1_Exo** follows this trend: Br < CN < NO with Br, CN, and NO_2 having activation barriers of 10.3, 11.5 and 11.6 kcal/mol, an increase by 1.0, 2.2, and 2.3 kcal/mol respectively.

Also, there is significant increase in activation barrier for the dinitrogen extrusion via **TS2_Endo** and **TS2_Exo** with Br having the least activation barriers of 31.2 and 37.0 kcal/mol and NO_2 having the highest activation barriers of 33.3 and 38.3 kcal/mol for **TS2_Endo** and **TS2_Exo** respectively.

In the experimental work of Chen et al[15], they observed that, when electron-withdrawing groups were substituted on the oxabicyclic alkene, the products yield decreased but with improved endo/exo selectivities (up to >99:1 endo/exo) and for the reaction of 4-nitrobenzenesulfonyl azide with di-substituted bromooxabicyclic alkene, only the endo product was isolated.

The decrease in product yield when electron-withdrawing groups are substituted at the position 6 and 7 of the oxabicyclic alkene can be attributed to the increase in activation barrier for **TS2** which is the rate-determining step, and the decrease in yield of the *exo* product isolated under the same

conditions can also be attributed to the increase in activation barrier for the cycloaddition step through **TS1_Exo**.

Effects of substituents on the reaction of 4-methoxybenzenesulfonyl azide with di-substituted oxabicyclic alkene was also investigated. From the results, electron-donating groups marginally decrease the activation barriers for **TS1_Endo** and **TS1_Exo** whiles electron-withdrawing groups marginally increase the activation barriers for the cycloaddition step through **TS1_Endo** and **TS1_Exo**. Also a marginal decrease in activation barrier is observed for **TS2_Endo** and **TS2_Endo** when electron-donating groups are substituted at the position 6 and 7 of the oxabicyclic alkene. However, electron-withdrawing groups increase the activation barrier for the dinitrogen extrusion step via **TS2_Endo** and **TS2_Exo** respectively.

Table 8. Activation energies of the elementary steps involved in the reaction of 4-nitrobenzenesulfonyl azide and several disubstituted oxabicyclic alkene, computed at the M06-2X/6-311+G(d,p) level of theory. Energies in kcal/mol

Substituents	**TS1_Endo**	**TS1_Exo**	**TS2_Endo**	**TS2_Exo**
H	16.8	9.3	30.2	35.8
CH_3	16.3	8.9	30.2	36.1
OH	12.0	4.2	30.7	36.6
NH_2	12.1	8.4	30.0	35.3
Br	14.4	10.3	31.2	37.0
CN	14.6	11.5	32.5	37.6
NO_2	13.7	11.6	33.3	38.3

Table 9. Relative energies intermediates and products involved in the reaction of 4-nitrobenzenesulfonyl azide and several disubstituted oxabicyclic alkene, computed at the M06-2X/6-311+G(d,p) level of theory. Energies in kcal/mol

Substituents	**1A + 2A**	**A_Endo**	**A_Exo**	**P_Endo**	**P_Exo**
H	0.0	-43.0	-45.0	-69.6	-73.1
CH_3	0.0	-44.2	-45.8	-70.6	-73.7
OH	0.0	-48.4	-50.4	-75.3	-78.4
NH_2	0.0	-45.3	-46.7	-70.0	-74.1
Br	0.0	-42.0	-43.2	-70.3	-71.9
CN	0.0	-40.9	-41.0	-67.4	-70.3
NO_2	0.0	-41.1	-40.8	-69.8	-70.1

Table 10. Activation energies of the elementary steps involved in the reaction of 4-methoxybenzenesulfonyl azide and several disubstituted oxabicyclic alkene, computed at the M06-2X/6-311+G(d,p) level of theory. Energies in kcal/mol

Substituents	TS1_Endo	TS1_Exo	TS2_Endo	TS2_Exo
H	17.2	10.7	32.9	39.1
CH_3	16.8	10.5	33.0	38.7
OH	16.6	10.4	33.5	39.5
NH_2	16.7	10.1	32.9	38.1
Br	17.4	11.0	33.8	39.8
CN	17.3	11.5	35.1	40.5
NO_2	17.1	11.6	35.8	40.7

Table 11. Relative energies of intermediates and products involved in the reaction of 4-methoxybenzenesulfonyl azide and several disubstituted oxabicyclic alkene, computed at the M06-2X/6-311+G(d,p) level of theory. Energies in kcal/mol

Substituents	1A + 2A	A_Endo	A_Exo	P_Endo	P_Exo
H	0.0	-41.9	-43.6	-67.8	-71.6
CH_3	0.0	-42.9	-44.2	-68.4	-72.1
OH	0.0	-47.2	-49.1	-73.3	-76.6
NH_2	0.0	-44.0	-44.9	-67.2	-72.5
Br	0.0	-41.3	-42.4	-68.3	-70.9
CN	0.0	-41.0	-40.8	-67.5	-70.0
NO_2	0.0	-41.3	-40.7	-68.5	-69.9

3.5 Reaction of oxabicyclic alkene with 2-nitrobenzenesulfonyl azide

Chen and co-workers observed that when 2 or 3-nitrobenzenesulfonyl chloride was used to generate the azide, the exo-cycloadducts were obtained as the predominant products whiles 4-nitrobenzenesulfonyl chloride gave the endo-cycloadducts as the predominant products. To provide insight into this varying selectivity when position of the substituent is varied, we employed 2-nitrobenzenesulfonyl azide and 2-methoxybenzenesulfonyl azide in our study.

The optimized geometries of the transition state structures as well as the relative energies of the reactants, intermediates, transition states and products involved in the reaction of 2-

nitrobenzenesulfonyl azide with oxabicyclic alkene are shown in Figure 3. In 2-nitrobenzenesulfonyl azide, the nitro group is substituted at the ortho position of the benzene. There appears to be no significant effect on the activation barriers leading to the formation of intermediates A_Endo and A_Exo via TS1_Endo and TS1_Exo respectively. Analysis of transition state structures of **TS2_Exo** reveal a significant decrease in activation barrier by 6.1 kcal/mol. The activation barrier of the cycloaddition step through **TS1_Endo** and **TS1_Exo** are 16.2 and 12.6 kcal/mol respectively. **TS1_Exo** is kinetically favored over **TS1_Endo** by 3.6 kcal/mol. Also, the activation barrier for the dinitrogen extrusion via **TS2_Endo** and **TS2_Exo** are 29.7 and 29.8 kcal/mol rendering this step less selective. Nevertheless, the overall formation of product **P_Exo** is kinetically and thermodynamically favoured over the formation of **P_Endo**. It can be argued that, the reason why the exo-cycloadducts is obtained as the predominant product is the significant decrease in activation barrier of the rate-determining step via **TS2_Exo**.

A similar observation is observed for the reaction of 2-methoxybenzenesulfonyl azide with benzenesulfonyl azide. A marginal decrease in activation barrier is observed for the cycloaddition step via **TS1_Endo** and **TS1_Exo**. The activation barrier for the dinitrogen extrusion via **TS2_Endo** and **TS2_Exo** are 35.0 and 37.4 kcal/mol indicating an increase by 2.1 kcal/mol and a decrease by 1.7 kcal/mol respectively. Hence, substituents at the position 2 of the benzenesulfonyl azide favor the formation of the exo-cycloadduct and disfavor the formation of the endo-cycloadducts as observed by Chen et al.[15].

Table 12. Activation energies and relative energies of intermediates and products involved in the reaction of 2-substitutedbenzenesulfonyl azide and oxabicyclic alkene, computed at the M06-2X/6-311+G(d,p) level of theory. Energies in kcal/mol

Substituent	**TS1_Endo**	**TS1_Exo**	**TS2_Endo**	**TS2_Exo**	**A_Endo**	**A_Exo**	**P_Endo**	**P_Exo**
NO_2	16.2	12.6	29.7	29.8	-38.9	-38.1	66.2	-73.1
OCH_3	16.7	10.3	35.0	37.4	-40.7	-42.1	-64.4	-69.8

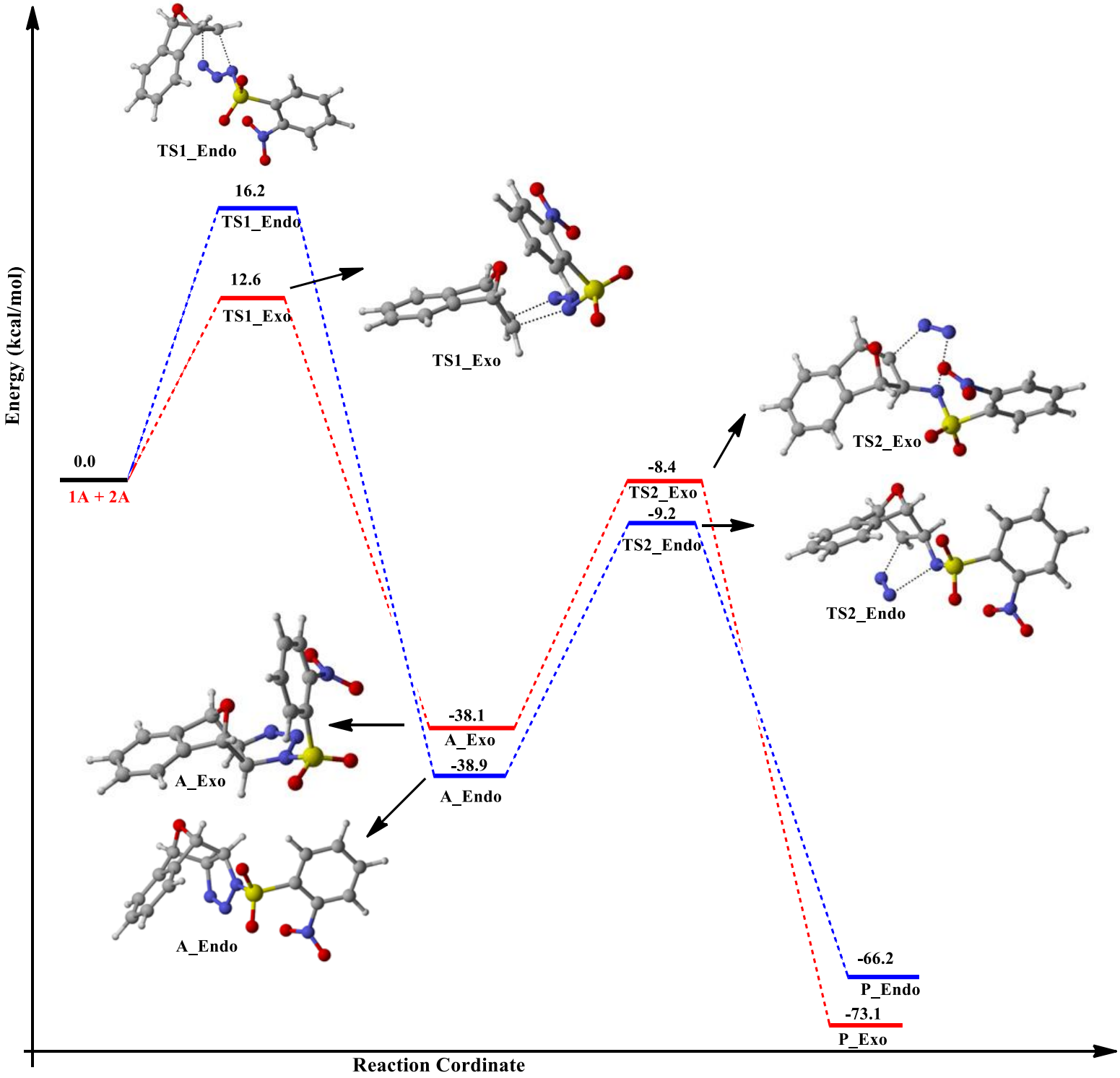

Figure 3. Zero point energy corrected Gibbs free energy profile for the reaction of Oxabicyclic alkene and 2-nitrobenzenesulfonyl azide to afford Aziridines P _Endo and P_Exo. All stationary points are optimized at the M06-2X/6-311G+(d,p) level of theory at 85 °C in gas phase. Relative energies in kcal/mol.

3.6 Normal versus inverse electron demand cycloaddition

Orbital interactions are important factors in determining the reactivity of 1,3-dipolar cycloaddition reactions. In this section, the frontier molecular orbital theory is applied to rationalize the reactivity of the 1,3-dipolar cycloaddition of reactants **1A** and **2A**. The possible orbital interactions are depicted in Figure 4.

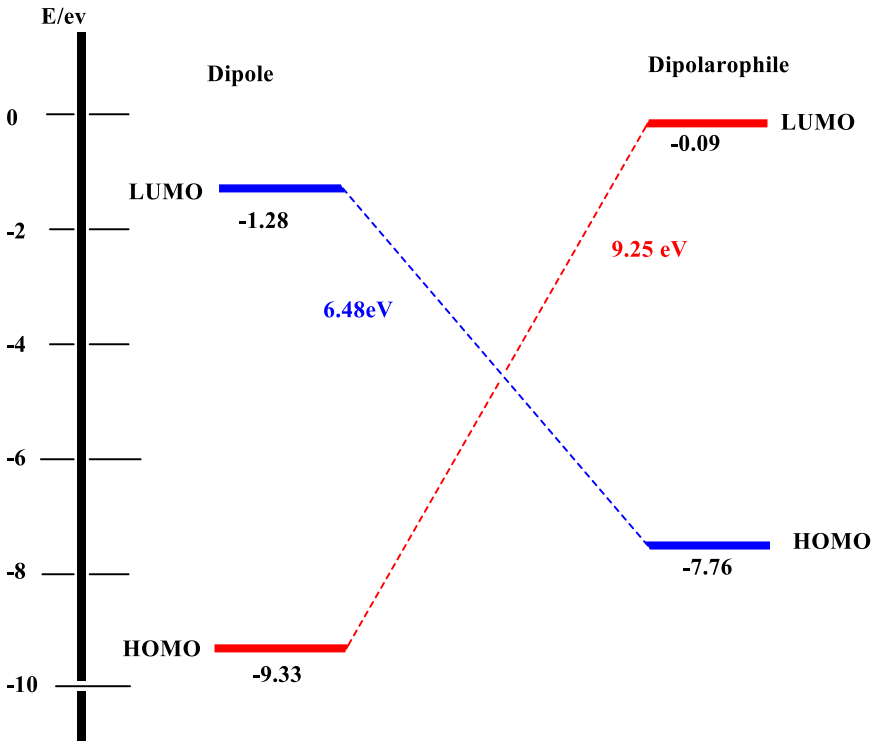

Figure 4. Frontier molecular orbital interactions in the 1,3-dipolar cycloaddition of oxabicyclic alkene and benzenesulfonyl azide at the M06-2X/6-311G+(d,p) level of theory.

The calculated HOMO and LUMO energy for the benzenesulfonyl azide which is the dipole are -9.33 eV and -1.28 eV respectively and that for the dipolarophile are -7.76 and -0.09 eV respectively (Figure 4). The energy gap for the HOMO $_{dipole}$ – LUMO $_{dipolarophile}$ is 9.25 eV and that of HOMO $_{dipolarophile}$ – LUMO $_{dipole}$ is 6.48 eV. The dominant pathway is the one which possess the smallest HOMO – LUMO energy gap. The analyses indicate that the dominant interactions occur between the HOMO of the dipolarophile and the LUMO of the dipole, and indication of an inverse

electron demand cycloaddition for the first step of Path A. In this case, the HOMO of the dipolarophile interacts with the low-lying LUMO of the dipole.

3.7 Analysis of the global reactivity indices

The electrophilicity indices is used as a parameter for predicting the chemical reactivity of electrophilic molecules. Molecules with the largest ω value will be the best nucleophile in a given series of molecules. Also, species with large ω values will be more reactive towards nucleophiles. From Table 13, the electrophilicities of the various substituted benzenesulfonyl azide derivatives are in the order NO_2 > CN > CF_3 > Cl > F > H > Ph > CH_3 > OCH_3 > OH > NH_2 with NO_2 being the most electrophilic species and hence more reactive towards the nucleophilic bicyclic alkene. The trends in activation energies for the initial [3+2] addition are consistent with the ω electrophilic index value.

Table 13. Global electrophilicities for the various substituted benzenesulfonyl azide. Orbital energies in electron volts (eV)

Substituent	HOMO	LUMO	μ	H	Ω	ΔN_{max}
H	-9.33	-1.28	-5.31	8.01	1.75	0.66
F	-9.32	-1.35	-5.34	7.98	1.78	0.67
Cl	-9.16	-1.47	-5.31	7.69	1.84	0.69
CF_3	-9.81	-1.75	-5.78	8.06	2.07	0.72
CN	-9.70	-2.09	-5.90	7.61	2.29	0.76
NO_2	-10.03	-2.56	-6.30	7.47	2.66	0.84
Ph	-8.37	-1.41	-4.89	6.96	1.72	0.70
CH_3	-9.01	-1.18	-5.09	7.83	1.66	0.65
OCH_3	-8.51	-1.07	-4.79	7.44	1.54	0.64
OH	-8.70	-1.13	-4.91	7.56	1.60	0.65
NH_2	-7.80	-0.96	-4.48	7.04	1.42	0.64

Conclusion

Two different pathways for the reaction of benzenesulfonyl azides with oxabicyclic alkenes have been investigated. The results of the study show that the most plausible pathway for the formation of the *endo* and *exo* aziridine products is through the initial [3+2] cycloaddition of the benzenesulfonyl azide with oxabicyclic alkene to form triazoline cycloadducts followed by dinitrogen extrusion instead of an initial dinitrogen cleavage from the benzenesulfonyl azide to form a nitrene species and subsequent insertion of this species into the olefinic bond of the oxabicyclic alkene proposed by Chen et al.[15]

The initial [3+2] addition of benzenesulfonyl azide with oxabicyclic alkene to afford triazoline intermediates is kinetically favored over the dinitrogen cleavage from benzenesulfonyl azide by 21.6 and 28.1 kcal/mol for *endo* and *exo* products respectively. Also the formation of intermediate aziridines is thermodynamically favored over the formation of the nitrene species by 54.3 (*endo)* and 55.3 (*exo*) kcal/mol. The dinitrogen extrusion step leading to the formation of *endo* aziridine isomer is kinetically favoured over that of *exo* isomer by 6.3 and 6.2 kcal/mol in gas phase and 1,4-dioxane respectively. Since the rate-determining step is the dinitrogen extrusion step, product *endo* aziridine isomer will be formed as the predominant product. Solvent 1,4-dioxane marginally decrease the activation barrier for dinitrogen extrusion step leading to the formation of both *endo* and *exo* aziridine product.

The ratio of *endo* aziridine product to *exo* product has been calculated using the Boltzmann distribution equation and the results obtained indicate an *endo* to *exo* ratio of 62:38 which is in excellent agreement with experiment (*endo* / *exo* = 67:33). The position of substituent on the benzenesulfonyl azide affects the *endo* / *exo* selectivity of the reaction. Substituents at the para-position of the benzenesulfonyl azide follow the observed diastereoselectivity of endo > exo whiles substituents at the ortho or meta-position would generate the *exo* cycloadduct as the predominant

product. Electron-donating groups on the oxabicyclic alkene decrease the activation barrier for the rate-determining step whiles electron-withdrawing groups increase the activation barrier for the rate-determining step. An FMO analysis shows an inverse electron demand nature for the reaction and results obtained are in complete agreement with experimental observation.

Acknowledgement

The authors are very grateful to the National Council for Tertiary Education, Republic of Ghana, for a research grant under the Teaching and Learning Innovation Fund (TALIF/KNUST/3/0008/2005), and to South Africa's Center for High Performance Computing for access to additional computing resource on the Lengau cluster.

Conflict of Interest

The authors declare that they have no conflict of interest whatsoever regarding the publication of this manuscript.

Supporting Information

The supporting Information file contains Cartesian coordinates of all optimized geometries, and absolute energies of all reactants, intermediates, transition states and products computed in this study.

ORCID

Daniel Aboagye Akuamoah: https://orcid.org/0000-0001-8285-973X

Richard Tia: https://orcid.org/0000-0003-1043-8869

Evans Adei: https://orcid.org/0000-0003-2544-8883

References

(1) Aggarwal, V. K.; Badine, D. M.; Moorthie, V. A. Asymmetric Synthesis of Epoxides and Aziridines from Aldehydes and Imines. *Aziridines and Epoxides in Organic Synthesis*. John Wiley and Sons: Weinheim January 9, 2006, pp 1–35. https://doi.org/10.1002/3527607862.ch1.

(2) Eum, H.; Choi, J.; Cho, C. G.; Ha, H. J. Regiochemistry-Directed Syntheses of Polyhydroxylated Alkaloids from Chiral Aziridines. *Asian J. Org. Chem.* **2015**, *4* (12), 1399–1409. https://doi.org/10.1002/ajoc.201500285.

(3) Kametani, T.; Honda, T. Application of Aziridines to the Synthesis of Natural Products. *Adv. Heterocycl. Chem.* **1986**, *39* (C), 181–236. https://doi.org/10.1016/S0065-2725(08)60765-5.

(4) Akhtar, R.; Naqvi, S. A. R.; Zahoor, A. F.; Saleem, S. Nucleophilic Ring Opening Reactions of Aziridines. *Molecular Diversity*. Springer International Publishing May 1, 2018, pp 447–501. https://doi.org/10.1007/s11030-018-9829-0.

(5) Cockrell, J.; Wilhelmsen, C.; Rubin, H.; Martin, A.; Morgan, J. B. Enantioselective Synthesis and Stereoselective Ring Opening of N-Acylaziridines. *Angew. Chemie - Int. Ed.* **2012**, *51* (39), 9842–9845. https://doi.org/10.1002/anie.201204224.

(6) McCoull, W.; Davis, F. A. ChemInform Abstract: Recent Synthetic Applications of Chiral Aziridines. *ChemInform* **2010**, *31* (46), no-no. https://doi.org/10.1002/chin.200046268.

(7) Tanner, D. Chiral Aziridines—Their Synthesis and Use in Stereoselective Transformations. *Angewandte Chemie International Edition in English*. March 31, 1994, pp 599–619. https://doi.org/10.1002/anie.199405991.

(8) Singh, G. S. Advances in Synthesis and Chemistry of Aziridines. In *Advances in Heterocyclic Chemistry*; Academic Press Inc., 2019; Vol. 129, pp 245–335. https://doi.org/10.1016/bs.aihch.2018.12.003.

(9) Hu, X. E. Nucleophilic Ring Opening of Aziridines. *Tetrahedron*. March 15, 2004, pp 2701–2743. https://doi.org/10.1016/j.tet.2004.01.042.

(10) Ismail, F. M. D.; Levitsky, D. O.; Dembitsky, V. M. Aziridine Alkaloids as Potential Therapeutic Agents. *European Journal of Medicinal Chemistry*. September 2009, pp 3373–3387. https://doi.org/10.1016/j.ejmech.2009.05.013.

(11) Liang, J.-L.; Yu, X.-Q.; Che, C.-M. Amidation of Silyl Enol Ethers and Cholesteryl Acetates with Chiral Ruthenium(Ii) Schiff-Base Catalysts: Catalytic and Enantioselective Studies. *Chem. Commun.* **2002**, No. 2, 124–125. https://doi.org/10.1039/B109272C.

(12) Klotz, K. L.; Slominski, L. M.; Hull, A. V; Gottsacker, V. M.; Mas-Ballesté, R.; Que, Jr., L.; Halfen, J. A. Non-Heme Iron(Ii) Complexes Are Efficient Olefin Aziridination Catalysts. *Chem. Commun.* **2007**, No. 20, 2063–2065. https://doi.org/10.1039/B700493A.

(13) Ochiai, M.; Miyamoto, K.; Hayashi, S.; Nakanishi, W. Hypervalent N-Sulfonylimino-Λ3-Bromane: Active Nitrenoid Species at Ambient Temperature under Metal-Free Conditions. *Chem. Commun.* **2010**, *46* (4), 511–521. https://doi.org/10.1039/B922033J.

(14) Ruppel, J. V; Jones, J. E.; Huff, C. A.; Kamble, R. M.; Chen, Y.; Zhang, X. P. A Highly Effective Cobalt Catalyst for Olefin Aziridination with Azides: Hydrogen Bonding Guided Catalyst Design. *Org. Lett.* **2008**, *10* (10), 1995–1998. https://doi.org/10.1021/ol800588p.

(15) Chen, S.; Yao, Y.; Yang, W.; Lin, Q.; Wang, L.; Li, H.; Chen, D.; Tan, Y.; Yang, D. Three-Component Cycloaddition to Synthesize Aziridines and 1,2,3-Triazolines. *J. Org. Chem.* **2019**, *84* (18), 11863–11872. https://doi.org/10.1021/acs.joc.9b01713.

(16) 18401 Von Karman Ave., # 370, Irvine, CA, 92715, U. Spartan, Wavefunction, Inc.

(17) Frisch, M. J.; Trucks, G. W.; Schlegel, H. B.; Scuseria, G. E.; Robb, M. A.; Cheeseman, J. R.; Scalmani, G.; Barone, V.; Mennucci, B.; Petersson, G. A. Gaussian 09, Revision b. 01, Gaussian. *Inc., Wallingford, CT* **2009**, *6492*.

(18) Zhao, Y.; Truhlar, D. G. Density Functionals with Broad Applicability in Chemistry. *Acc. Chem. Res.* **2008**, *41* (2), 157–167. https://doi.org/10.1021/ar700111a.

(19) Paton, R. S.; Steinhardt, S. E.; Vanderwal, C. D.; Houk, K. N. Unraveling the Mechanism of Cascade Reactions of Zincke Aldehydes. *J. Am. Chem. Soc.* **2011**, *133* (11), 3895–3905. https://doi.org/10.1021/ja107988b.

(20) Paton, R. S.; Mackey, J. L.; Kim, W. H.; Lee, J. H.; Danishefsky, S. J.; Houk, K. N. Origins of Stereoselectivity in the *Trans* Diels−Alder Paradigm. *J. Am. Chem. Soc.* **2010**, *132* (27), 9335–9340. https://doi.org/10.1021/ja1009162.

(21) Jacopo Tomasi, Benedetta Mennucci, and R. C. Quantum Mechanical Continuum Solvation Models. *Chem. Rev.* **2005**, *105* (8), 2999–3094. https://doi.org/10.1021/CR9904009.

(22) Clark, M.; Cramer, R. D.; Van Opdenbosch, N. Validation of the General Purpose Tripos 5.2 Force Field. *J. Comput. Chem.* **1989**, *10* (8), 982–1012. https://doi.org/10.1002/jcc.540100804.

(23) Opoku, E.; Tia, R.; Adei, E. Computational Studies on [4 + 2] / [3 + 2] Tandem Sequential Cycloaddition Reactions of Functionalized Acetylenes with Cyclopentadiene and Diazoalkane for the Formation of Norbornene Pyrazolines. *J. Mol. Model.* **2019**, *25* (6), 168. https://doi.org/10.1007/s00894-019-4056-x.

(24) Opoku, E.; Tia, R.; Adei, E. [3 + 2] versus [2 + 2] Addition : A Density Functional Theory Study on the Mechanistic Aspects of Transition Metal-Assisted Formation of 1 , 2-Dinitrosoalkanes. *J. Chem.* **2016**, *2016* (7). https://doi.org/10.1155/2016/4538696.

(25) Domingo, L. R.; Aurell, M. J.; Patricia Pérez, A.; Renato Contreras. Quantitative Characterization of the Local Electrophilicity of Organic Molecules. Understanding the Regioselectivity on Diels−Alder Reactions. *J. Phys. Chem.* **2002**, *106* (29), 6871–6875. https://doi.org/10.1021/JP020715J.

(26) Parr, R. G.; Szentpály, L. v.; Liu, S. Electrophilicity Index. *J. Am. Chem. Soc.* **1999**, *121* (9), 1922–1924. https://doi.org/10.1021/ja983494x.

(27) Koopmans, T. Über Die Zuordnung von Wellenfunktionen Und Eigenwerten Zu Den Einzelnen Elektronen Eines Atoms. *Physica* **1934**, *1* (1–6), 104–113. https://doi.org/10.1016/S0031-8914(34)90011-2.

Graphical Abstract